AIAA Propulsion and Energy Forum
August 9-11, 2021, VIRTUAL EVENT
AIAA Propulsion and Energy 2021 Forum

10.2514/6.2021-3719



# A one-dimensional transient calculation method for flow instability of supercritical hydrocarbon in cooling channels

Yichao Jin[1], Kun Wu[2], Yang Lu[3], Xuejun Fan[4]

*State Key Laboratory of High Temperature Gas Dynamics, Institute of Mechanics, Chinese Academy of Sciences, Beijing 100190, People's Republic of China*

*School of Engineering Science, University of Chinese Academy of Sciences, Beijing 100049, People's Republic of China*



**The flow instability in the regenerative cooling channels is one of the important issues for the thermal protection of hypersonic scramjet engines. Taking into account the dynamic process of the heat transfer and flow instability, a one-dimensional transient model with several associated modules including the cracking reaction, convective heat transfer, and calculation of physical properties has been developed to investigate the flow instability characteristics of the supercritical hydrocarbon fuel in the cooling channels. The calculated results were compared and validated against the available experiments and numerical benchmarks attaining good agreements. Moreover, the influence of the external driving pressure drop on the in-tube flow was further investigated. The results shows that the right intersection point of the two characteristic curves leads to stable state, while the characteristics of the left equilibrium point is related to the external driving pressure drop. In addition, it is also observed that under a certain range of the pressure drop, the in-tube flow may transfer from the left equilibrium point to the right one then stabilize at the right equilibrium point.**

## Nomenclature

| | | |
|---|---|---|
| $A$ | = | section area |
| $C_p$ | = | heat capacity |
| $d$ | = | diameter of the channel |
| $E$ | = | internal energy |
| $H$ | = | enthalpy |
| $h_{tc}$ | = | convection heat transfer coefficient |
| $k$ | = | thermal conductivity |
| $k_F$ | = | chemical reaction rate |
| $L$ | = | length |
| $m$ | = | flow rate |
| $Nu$ | = | Nusselt number |
| $p$ | = | pressure |
| $Pr$ | = | Prandtl number |
| $q$ | = | heat flux |
| $S$ | = | perimeter of the channel |
| $T$ | = | temperature |
| $t$ | = | time |
| $u$ | = | velocity |
| $x$ | = | Cartesian coordinate in the $x$ direction |
| $Y$ | = | mass fraction |

[1] PhD student, Institute of Mechanics (CAS), jinyichao@imech.ac.cn
[2] Associate Professor, Institute of Mechanics (CAS), wukun@imech.ac.cn
[3] Associate Professor, Institute of Mechanics (CAS), luyang@imech.ac.cn
[4] Professor, Institute of Mechanics (CAS), xfan@imech.ac.cn, AIAA lifetime member (Corresponding author).

$\lambda$ = friction coefficient
$\xi, \eta, \zeta$ = coordinates
$\rho$ = density

*Subscripts*
$b$ = bulk
$c$ = cracking reaction
$F$ = fuel
$f$ = fluid
$w$ = solid wall



## I. Introduction

Flow instabilities induced by thermal load have been an important issue in the design and operation of industrial systems, such as steam generation [1], nuclear reactors [2] and electronic cooling systems [3]. Recently, the instability phenomena in regenerative cooling systems [4] are also of great interest because of the world-wide development of scramjet engines. During the cooling process, the hydrocarbon coolant may undergo phase change which leads to heat transfer deterioration [5] and even flow instability [4, 6]. Especially, for cooling systems constitute several parallel pipes, a locally germinated small perturbation could finally induce flow excursion under certain positive feedback, which severely affects the reliability of the cooling system.

Flow excursion, also known as Ledinegg instability, was first introduced by Ledinegg [7], which roots in the multi-valued hydrodynamic characteristics of its internal characteristic line, namely the pressure drop-mass flow rate characteristic line. The classical method which has been used to study Ledinegg instability is linear stability analysis. In this approach, small perturbation linearization theory is exploited to determine the stability of the equilibria between two characteristic lines [8]. By comparing the slope at multiple intersection points, the one in the negative slope region of the internal characteristic line is regarded to be unstable and vice versa [9-10]. However, the Ledinegg instability could also be coupled with a dynamically unstable flow such as density-wave instability [11] and pressure-drop instability [12]. For these complicated flows, linear analysis becomes inadequate as strong nonlinearity is involved and transient numerical calculation approaches are more attractive.

Recently, several one-dimensional models based on the time domain analysis have been reported in two-phase flows. Munoz-Cobo et al. [13] have established a reduced-order model to investigate the variations of pressure drop and inlet mass flux when out of phase oscillations take place. Schlichting et al. [12] utilized a transient lumped parameterized model to investigate the dynamics of pressure-drop and density-wave oscillations. In the aforementioned models, flow along the channel is simply divided into two sections based on the boiling boundary, which may be oversimplified for predicting the dynamics of hydrocarbon flow in cooling channels. Recently, more accurate one-dimensional methods were proposed in which more discrete subsections were incorporated to improve prediction accuracy. Lee et al.[14] and Yun et al. [15] respectively studied two-phase flow instability in a parallel multi-channel system based such one-dimensional models. As for supercritical flow, Chen et al. [16], Lu et al. [17] and Ruspini et al. [18] also have developed more complex one-dimensional methods using various numerical discretization methods.

It is obvious from the above brief review, the previous studies are mainly concerned with conventional fluids, such as water and carbon dioxide, while the relevant work in supercritical hydrocarbon fuels is relatively rare. Besides, the physical properties of hydrocarbon fuels are very complicated due to their diverse components, which leads to notable uncertainty in modeling and expensive cost in calculation. Especially, the crack reactions that arise under high temperature will aggravate the challenge of calculation, which leads to a more complicated multi-valued hydrodynamic problem. Therefore, it is essential to establish a one-dimensional transient calculation framework to attain an in-depth understanding of the instability behaviors of supercritical hydrocarbon flow in cooling channels of regenerated cooling engines. In the present work, a one-dimensional transient calculation framework is proposed and validated for hydrodynamic instability in a single channel under supercritical operating conditions. Then, the dynamic characteristics are further investigated for the cooling channel under various operating conditions.

## II. Numerical methodology

The theoretical formulation of the proposed numerical framework is briefly elaborated in this section. The conservation equations for one-dimensional flow are summarized as:

$$\frac{\partial \rho}{\partial t} + \frac{\partial \rho u}{\partial x} = 0 \tag{1}$$

$$\frac{\partial \rho u}{\partial t} + \frac{\partial \rho u u}{\partial x} = -\frac{\partial p}{\partial x} - \frac{\lambda \rho u^2}{2d} \tag{2}$$

$$\frac{\partial \rho E}{\partial t} + \frac{\partial \rho u H}{\partial x} = \frac{\dot{q}_w S}{A} + \dot{q}_c \tag{3}$$

$$\frac{\partial \rho Y_F}{\partial t} + \frac{\partial \rho u Y_F}{\partial x} = -k_F \cdot \rho Y_F \tag{4}$$

where $\rho$ is the density, $u$ the flow velocity, $p$ the pressure, $E$ the total internal energy, $H$ the total enthalpy, $\lambda$ the friction coefficient, $S$ the perimeter of the channel and $A$ the cross section area. The $\dot{q}_w$ is the surface heat flux, and $\dot{q}_c$ is the heat release or absorption due to cracking reactions.

### A. Solution procedure of fluid flow

To solve the above nonlinear partial differential equations, the semi-implicit scheme with collocated grid is adopted to discretize the governing equations as shown in Fig. 1. The way how each governing equation is discretized will be detailed in the following.

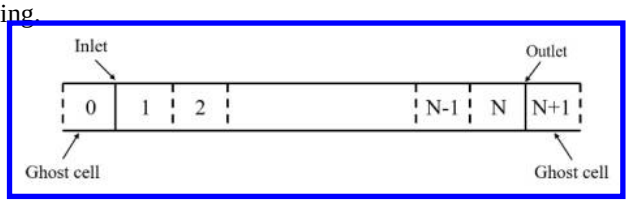


**Fig. 1. Collocated grid for semi-implicit scheme**

a) Mass conservation equation:

$$\frac{\rho_i^{j+1} - \rho_i^j}{\Delta t} \Delta V_i + F_{f,i} - F_{f,i-1} = 0 \tag{5}$$

where $\Delta V_i$ is the cell volume, $F_{f,i}$ is calculated as $F_{f,i} = 0.5(\rho_i u_i + \rho_{i+1} u_{i+1})A$ .

b) Momentum conservation equation:

$$\frac{\rho_i^{j+1} u_i^{j+1} - \rho_i^j u_i^j}{\Delta t} \Delta V_i + F_{f,i} \frac{u_i^{j+1} + u_{i+1}^{j+1}}{2} - F_{f,i-1} \frac{u_{i-1}^{j+1} + u_i^{j+1}}{2} = p_{f,i-1} A - p_{f,i} A - \frac{\lambda_i \rho_i^j u_i^j u_i^j \Delta L_i}{2d} A \tag{6}$$

Rearranging the above formula:

$$A_{i,1} u_{i-1}^{j+1} + A_{i,2} u_i^{j+1} + A_{i,3} u_{i+1}^{j+1} = B_{i,u} + B_{i,p} \tag{7}$$

where $A_{i,1} = -\frac{F_{f,i-1}}{2}$, $A_{i,2} = \left( \frac{\rho_i^{j+1} \Delta V_i}{\Delta t} - \frac{F_{f,i-1}}{2} + \frac{F_{f,i}}{2} \right)$, $A_{i,3} = \frac{F_{f,i}}{2}$. $B_{i,u}$ involves the explicit form of velocity, calculated as $B_{i,u} = \frac{\rho_i^j u_i^j \Delta V_i}{\Delta t} - \frac{\lambda_i \rho_i^j u_i^j u_i^j \Delta L_i}{2d} A$, and $B_{i,p}$ denotes the source term induced by pressure difference expressed as $B_{i,p} = (p_{f,i-1} - p_{f,i})A$. The friction coefficient $\lambda$ is obtained by the Blasius' correlation [19].

c) Energy conservation equation:

$$\frac{\rho_i^{j+1} E_i^{j+1} - \rho_i^j E_i^j}{\Delta t} \Delta V_i + F_{f,i} \frac{H_i^{j+1} + H_{i+1}^{j+1}}{2} - F_{f,i-1} \frac{H_{i-1}^{j+1} + H_i^{j+1}}{2} = \dot{q}_w S \Delta L_i + \dot{q}_c \Delta V_i \tag{8}$$

In the present work, the NIST SUPERTRAPP is utilized to calculate the thermal properties of the hydrocarbon fuels. To facilitate the formulation of the equation of state, temperature and pressure are regarded as independent thermodynamic variables. Subsequently, the density and enthalpy can be linearized by the equation of state as:

$$\rho_i^{j+1} - \rho_i^j = \left(\frac{\partial \rho}{\partial p}\right)_i^j \Delta p_i + \left(\frac{\partial \rho}{\partial T}\right)_i^j \Delta T_i \tag{9}$$

$$\rho_i^{j+1} E_i^{j+1} - \rho_i^j E_i^j = \left(H\frac{\partial \rho}{\partial p} + \rho\frac{\partial H}{\partial p} - 1\right)_i^j \Delta p_i + \left(H\frac{\partial \rho}{\partial T} + \rho\frac{\partial H}{\partial T}\right)_i^j \Delta T_i \tag{10}$$

After substituting Eqs. (9)- (10) into mass and energy equations, a combined matrix form can be obtained:

$$\begin{pmatrix}\Delta p \\ \Delta T\end{pmatrix}_i^j = \frac{\Delta t}{\Delta V_i}\left(\Phi_i^i\right)^{-1}\begin{pmatrix}DF1 \\ DF2\end{pmatrix} \tag{11}$$

where

$$\Phi_i^j = \begin{pmatrix} \frac{\partial \rho}{\partial p} & \frac{\partial \rho}{\partial T} \\ H\frac{\partial \rho}{\partial p} + \rho\frac{\partial H}{\partial p} - 1 & H\frac{\partial \rho}{\partial T} + \rho\frac{\partial H}{\partial T} \end{pmatrix}_i^j$$

$$DF1 = F_{f,i-1} - F_{f,i}$$

$$DF2 = F_{f,i-1}\frac{H_{i-1}^{j+1} + H_i^{j+1}}{2} - F_{f,i}\frac{H_i^{j+1} + H_{i+1}^{j+1}}{2} + \dot{q}_w \mathrm{S}\Delta L_i + \dot{q}_c \Delta V_i$$

The above method is essentially a pressure-based algorithm, and the linear central scheme may lead to checkerboard problem in the pressure field. Therefore, the Rhie-Chow interpolation scheme [20] is employed in this work to eliminate the pressure wave.

### B. Cracking model

Hydrocarbon fuel is a complex mixture with a large number of components, which leads to complex chemical mechanism consisting of hundreds of species and reactions. However, to emphasis on the characteristics of flow instability instead of the detailed chemical kinetic process, the *n*-decane is considered as the surrogate fuel. In addition, the proportional product distribution (PPD) assumption [22] is used to describe the pyrolysis reaction as in Eq.(4). $Y_F$ is the mass fraction of reactant, and $k_F$ is the chemical reaction rate obtained using the Arrhenius relation. The overall reaction is specifically expressed as follows [22]:

$$\begin{gathered} C_{10}H_{22} \rightarrow 0.153CH_4 + 0.222C_2H_4 + 0.138C_2H_6 + 0.200C_3H_6 \\ +0.185C_3H_8 + 0.171C_4H_8 + 0.118C_4H_{10} + 0.149C_5H_{10} \\ +0.137C_5H_{12} + 0.170C_6H_{12} + 0.106C_6H_{14} + 0.147C_7H_{14} \\ +0.091C_7H_{16} + 0.132C_8H_{16} + 0.040C_8H_{18} + 0.046C_9H_{18} + 0.031C_9H_{20} \end{gathered} \tag{12}$$

### C. Calculation of the thermal and transport properties

For complex hydrocarbon fuels, the calculations of thermodynamic and transport properties usually occupy more than 80% of the total CPU time, so it is essential to reduce the cost of thermal properties calculation. To facilitate an efficient calculation, a look-up table method is applied in present paper. First, the thermal and transport properties of the mixture are evaluated prior to the simulation and stored in a three-dimensional library (pressure *p*, temperature *T*, and mass fraction of reactant *Y*). Then, for each inquiry point $(p_q, T_q, Y_q)$, the average value of the eight points in its nearest vicinity are used to improve numerical accuracy, and the calculation of physical properties are outlined in Fig. 2. In the present work, the interval of pressure, temperature and mass fraction are $\Delta p = 0.01$ MPa, $\Delta T = 2$ K, and $\Delta Y = 0.01$, respectively.

$$\xi = \frac{p - p_{min}}{\Delta p}, \eta = \frac{T - T_{min}}{\Delta T}, \zeta = \frac{Y - Y_{min}}{\Delta Y} \tag{13}$$

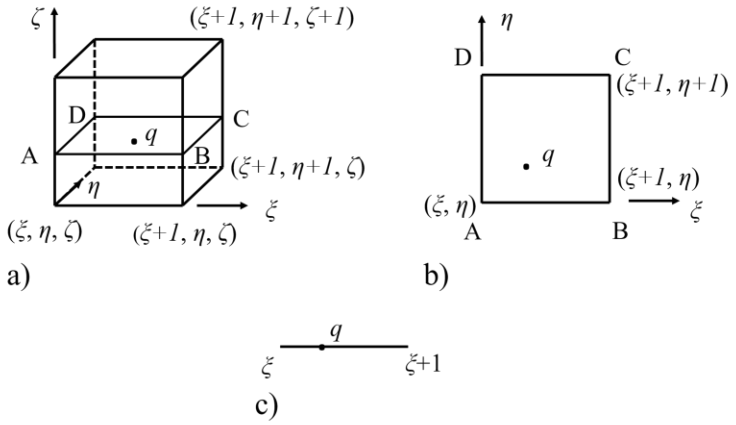


**Fig. 2. Schematic diagram of thermal and transport properties calculation**

### D. Approach for updating the inlet flow rate

Affected by pressure feedback, the flow rate in the channel varies with time. In the previous study [21], the "Regula-Falsi" method was used to update the inlet flow rate. However, this method is wasteful in the multi-channel parallel system due to a mass of guessed calculations. Thereby, a more practical model has been proposed to solve the feedback relation between the pressure and inlet flow rate. Referring to the model in Ref. [23], the cooling system is divided into two parts, namely the connect channel and heated channel, as schematized in Fig. 3. The inlet pressure $p_1$ and the exit pressure $p_3$ are prescribed, whereas the inlet pressure of the heated section $p_2$ varies from time to time. Integrated over the connect channel from 0 to $L_1$, a lumped model can be obtained from the following momentum equation:

$$\frac{L_1}{A}\frac{dm}{dt} = p_1 - p_2 - \frac{\lambda\rho u^2 L_1}{2d} = p_1 - p_3 - (p_2 - p_3) - \frac{\lambda\rho u^2 L_1}{2d} = \Delta p_t - \Delta p - \frac{\lambda\rho u^2 L_1}{2d} \tag{14}$$

where, $\Delta p_t$ is the external driving force, and $\Delta p$ is the pressure drop in the heated channel, which is calculated from the fluid flow module.

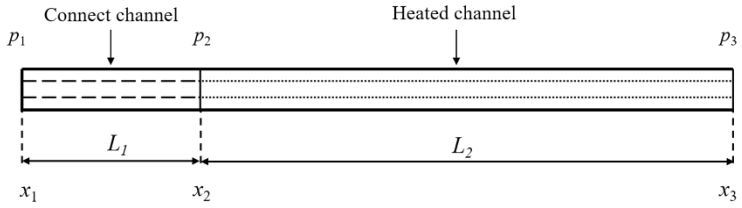


**Fig. 3. Schematic diagram of the cooling channel along with the connect channel**

Based on the above numerical algorithms, an in-house code was developed to perform the calculation and then employed to investigate the instabilities of hydrocarbon fuel in cooling channel under supercritical conditions. To clarify the calculation process, the flowchart of the proposed calculation framework is summarized in Fig. 4.

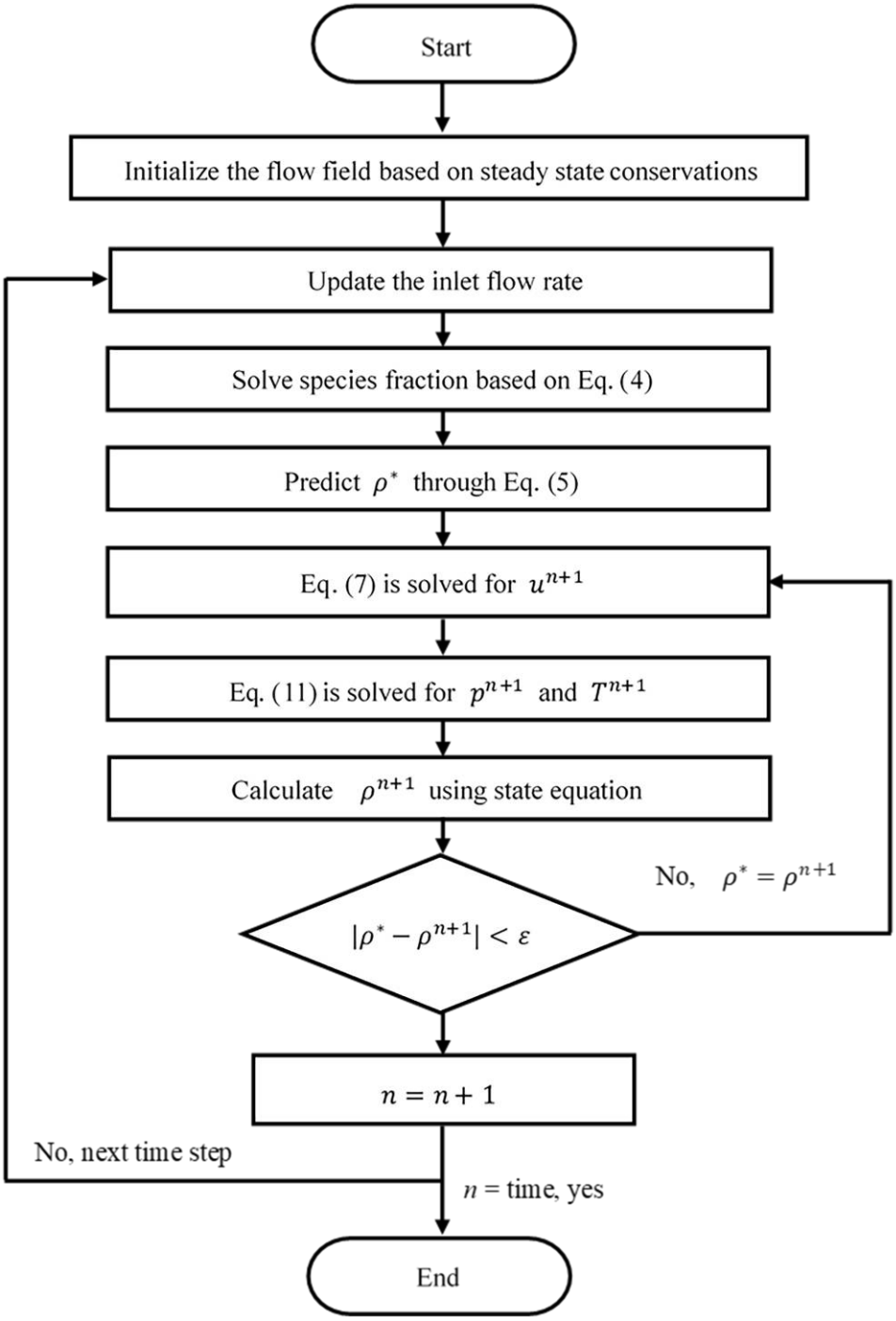


**Fig. 4. Diagram of the numerical calculation framework.**

## III. Model validations

The heated channel flow using hydrocarbon as coolant is extremely complicated, involving various physical issues such as real-fluid effect, flow instability, heat transfer, and cracking reaction. To validate the reliability and accuracy of the new solver for those aforementioned issues, a series of test calculations have been carried out as below.

### A. Look-up table method

Fig. 5 compares the results obtained by direct calculation with the SUPERTRAPP and the look-up table method under a cracking conversion rate of 32%. Compared to the direct calculation subroutine, a speedup ratio of around 50 has been achieved in present work. It is also clear that the excellent agreements between the two methods are obtained. The maximum relative error of the two methods is within 0.5%, which implies that the look-up table method gains acceptable accuracy.

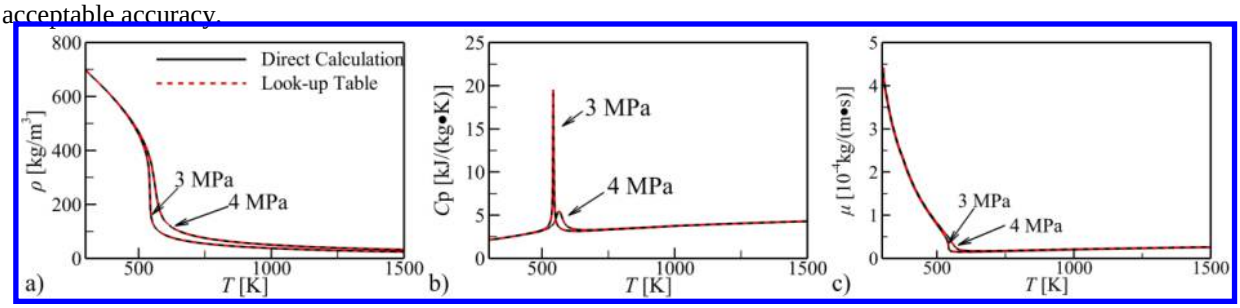


**Fig. 5. Comparisons between the direct calculation and the look-up table method: a) density, b) heat capacity and c) viscosity**

### B. Pressure drop in the channel

Referring to the experiments of Yang et al. [4], a circular tube with an internal diameter of 2 mm and the length of 670 mm is adopted as benchmark. The corresponding critical parameters of the coolant are summarized in Table 1. As presented in Fig. 6, it shows that the calculated results agree well with the experimental measurements, expect that the pressure drop is slightly underestimated in the small mass flow rate range. Overall, the positive and negative slope regions can be clearly distinguished in the calculation, and the stability boundaries are in consistent with the experimental observation. Thus, the capability of the present numerical framework in capturing the multi-valued hydrodynamic characteristics is validated.

**Table 1. Mass fraction and critical parameter of the fuels**

| Fuel | Mass fraction (%) | | Critical point | |
|---|---|---|---|---|
| | Pentane | Cyclohexane | Pressure (MPa) | Temperature (K) |
| Mix 1 | 100 | 0 | 3.37 | 469.75 |
| Mix 2 | 30 | 70 | 3.60 | 491.60 |

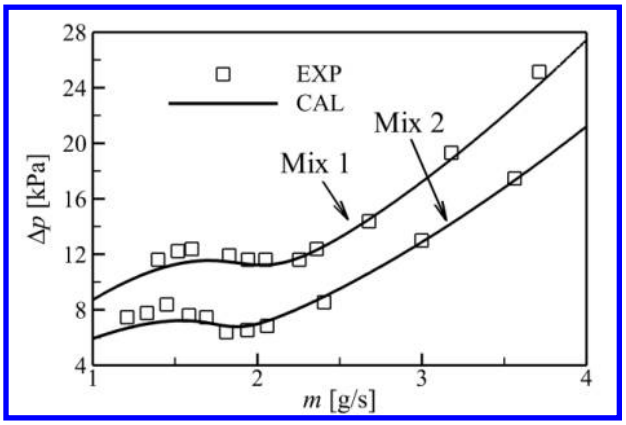


**Fig. 6. Comparison between the present calculations and the experimental data at 4.5 MPa [4].**

### C. Cracking reaction

In this section, the model validation was conducted by following the experiment of Ward et al. [22]. The tube is 0.5 mm in diameter and 375 mm in length, and the flow conditions of this experiment are listed in Table 2. The heat flux absorbed from the wall is calculated through the following formula:

$$q_w = h_{tc}(T_w - T_f) \tag{15}$$

where $h_{tc} = Nu \cdot k/d$. $N_u$ is Nusselt number which is obtained by the modified Dittus-Boelter correlation:

$$Nu = 0.023 Re_f^{0.8} Pr_f^{0.4} (\frac{T_f}{T_w})^{0.11} \tag{16}$$

In Eq. (16), $Re_f$ is the Reynolds number, $Pr_f$ the Prandtl number, $T_f$ the temperature of the coolant, and $T_w$ the wall temperature. The transient model is concerned with fluid flows and heat transfer of *n*-decane with mild endothermic pyrolysis in a mini tube. Variations of conversion rate, bulk temperature, and fluid mixture density of *n*-decane are depicted in Fig. 7. The predicted results are quite consistent with experiment data under the operating conditions.

**Table 2. Flow conditons of the experiment**

| Flow rate (m*L*/min) | Inlet temperature (K) | Operating pressure (MPa) | Maximum wall temperature (K) |
|---|---|---|---|
| 0.5 | 423.15 | 3.45 | 874 |

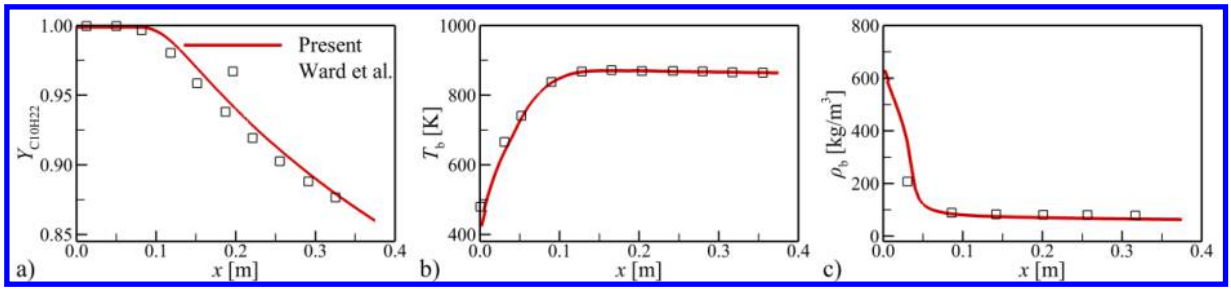


**Fig. 7. Comparison between simulation and experiment data [22]: a) mass fraction of n-decane, b) bulk temperature and c) density**

### D. Unsteady flow and heat transfer

To verify the simulation performance on unsteady flow of the present model, the bulk temperature of methane in a heated channel is monitored. The test case follows the work in Ref. [24], in which the diameter of heated tube is 2 mm and the length is 300 mm. Moreover, the inlet velocity is 25.0 m/s, inlet temperature is 120 K, the exit pressure is 8.0 MPa, and the heated power ranges from 3 to 7 MW/m$^2$. Three different cases are simulated in this section, and the sampling point is in the middle of the heated channel. Despite its simplicity, the model agrees well with the simulation data by Ruan et al. [24], which indicates that the proposed numerical framework can faithfully capture the dynamical response to the heating perturbation.

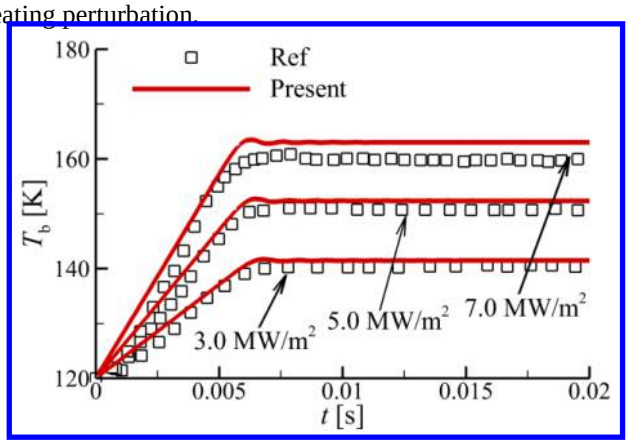


**Fig. 8. Comparison between the numerical simulation and reference data [24]**

## IV. Results and discussion

By employing the validated numerical framework, the flow dynamics in a single cooling channel are investigated under various operating conditions. Before the system response under specific driving pressure drop can be evaluated, it is helpful to first determine the characteristics of its steady state. In Fig.9, the pressure drop along a single horizontal pipe is demonstrated as a function of the flow rate, whose geometric and operating conditions are summarized in Table 3. Due to the drastic change of fluid density under supercritical conditions, there exists a negative slope region in the internal characteristic curve, which poses the multi-valued phenomenon in heated channel flows. To facilitate the descript of the stability patterns, the internal characteristic curve is divided into three parts, namely left branch, right branch, and negative slope region as can be seen in Fig. 9(a). As illustrated in Fig. 9(b), there are three intersection points between the internal and external characteristic curves with the operating point $P$ being unstable. Correspondingly, a slight disturbance in mass flow rate will lead to a spontaneous shift to left equilibrium point $P'$or right equilibrium point $P''$. This phenomenon involving a sudden change in the flow rate is the well-known Ledinegg instability.

However, due to the flow hysteresis, the actual flow at equilibrium point may not closely conform the prediction obtained by the linear analysis. Therefore, the transient flow processes of the cooling channel deviating from the initial equilibrium position are conducted based on the present model, and the effect of external driving force is also studied. In this paper, the original state of cooling channel is initialized using the steady flow of mass flow rate 2.5 g/s, which is approximately at the maximum in the internal characteristic curve. And the concerned external driving pressure drops are respectively 12.0 kPa, 11.0 kPa, 10.8 kPa, 10.5 kPa, 10.4 kPa, 10.2 kPa, 10.1 kPa and 10.0 kPa.

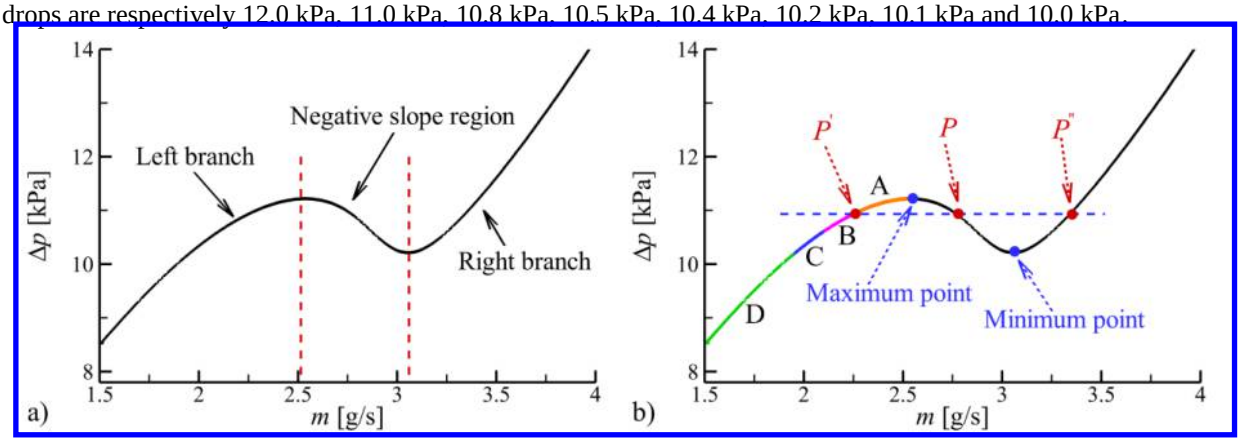


**Fig. 9. a) Internal curve and b) The intersection points between internal and external curves.**

**Table 3. Simulation conditions for the heated circular tube**

| Diameter (mm) | Connect length (mm) | Heated length (mm) | Inlet temperature (K) | Outlet pressure (MPa) | Heat flux ($MW/m^2$) |
|---|---|---|---|---|---|
| 2.0 | 100 | 500 | 300 | 3.0 | 1.0 |

From the transient processes of the mass flow rate as shown in Fig. 10, it is clear that the external driving pressure drop has a significant influence on the in-tube flow. On the equilibrium curve above the maximum point, there only exists one intersection point between two characteristic curves. Thus, the flow rate in the channel is attracted to this operating point, and finally stabilizes at the right equilibrium point, as Fig. 10(a) . For the flow in the left branch, it is complicated and related to the external driving force. As the external driving force decreases, the trajectory of the flow rate transfers from a stable node to a limit cycle. To describe the channel flow in detail, the equilibrium curve for the steady-state solution is divided into four regions namely A, B, C, and D, as displayed in Fig. 9(b).

1) **Region A:** In this region, the intrinsic mass flow rate and pressure drop are relative lower than those of the maximum point. Due to the lower driving force, the flow rate of the cooling channel decreases, and then converge towards the left equilibrium point within a short time delay as can be seen in Fig 10(b) and (c).

2) **Region B:** Compared to the Region A, the difference between the driving force and initial pressure drop becomes larger, and the dynamic instability appears in the channel, see the examples in Fig. 10(d) and (e). The flow rate decreases first, and then flow oscillation starts after the flow excursion. The magnitude of oscillation grows to a

certain value and then remains unchanged. Therefore, the trajectories converge to a stable limit cycle. Besides, the oscillation's amplitude increases but the frequency decreases, as the external driving force decreases.

3) **Region C:** Compared to the flow in Region B, the oscillation's amplitude of the flow rate becomes larger. If observing from the internal characteristic curve, the operating state can shift from left branch to the right one. Therefore, after being fully developed, the cooling channel may stabilize at the right equilibrium point, such as Fig. 10 (f).

4) **Region D:** The pressure drop is lower or slightly higher than the minimum of the internal characteristic curve. The flow rate can also cross the negative slope region and reach the right branch, but the right equilibrium point is so close to the minimum position, or nonexistent. Under the action of the dynamic feedback of the system, it can no longer stabilize at the right branch of characteristic curve. Hence, a low-frequency flow oscillation with relatively large amplitude emerges, such as Fig. 10 (g) and (h). Moreover, the oscillation's amplitude and frequency increase with the decrease in the external driving force.

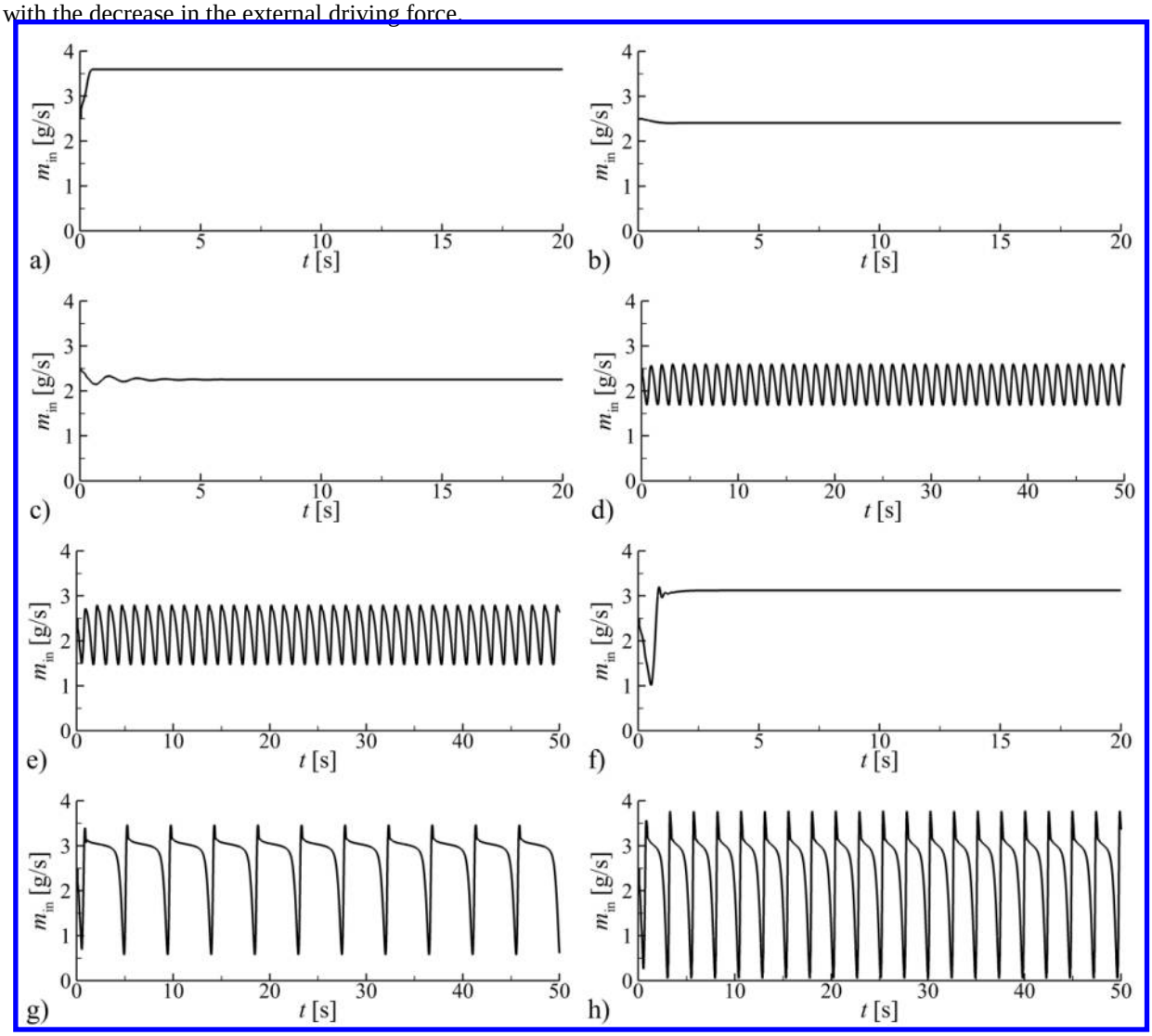


**Fig. 10. Temporal evolution of the mass flow rate under various driving pressure drops of a) 12.0 kPa, b) 11.0 kPa, c) 10.8 kPa, d) 10.5 kPa, e) 10.4 kPa, f) 10.2 kPa, g) 10.1 kPa and h) 10.0 kPa**

Obviously, the results obtained by transient model is not identical to the ones predicted by linear analysis based on the quasi-steady state assumption. Especially, there exists a certain range in internal characteristic curve, where the mass flow rate can oscillate from the left equilibrium point to the right one, and finally stabilizes at the right branch. This phenomenon has rarely been reported in the previous literatures.

To further illustrate the temporal evolution of the channel flow, a detailed discussion on several typical conditions is presented. Three operations with driving pressure drops of 10.4 kPa, 10.2 kPa and 10.1 kPa are compared as shown

in Fig. 11. The limit cycle composed of inlet and outlet flow rate could be divided to three stages. First, both the inlet and outlet flow rates decrease, nevertheless the former to a larger extend. Second, the inlet flow rate increases, while the outlet flow rate continues to reduce. Third, the outlet flow rate raises rapidly, whereas the flow rate at the inlet declines slightly. In the third stage of the flow evolution, the mass flow rate in the entire channel remains the same level in a short period, which can be approximated as a steady state of the internal characteristic curve. If its pressure drop is smaller than the external driving force, the flow rate can overshoot to the right equilibrium point and stabilize at right branch.

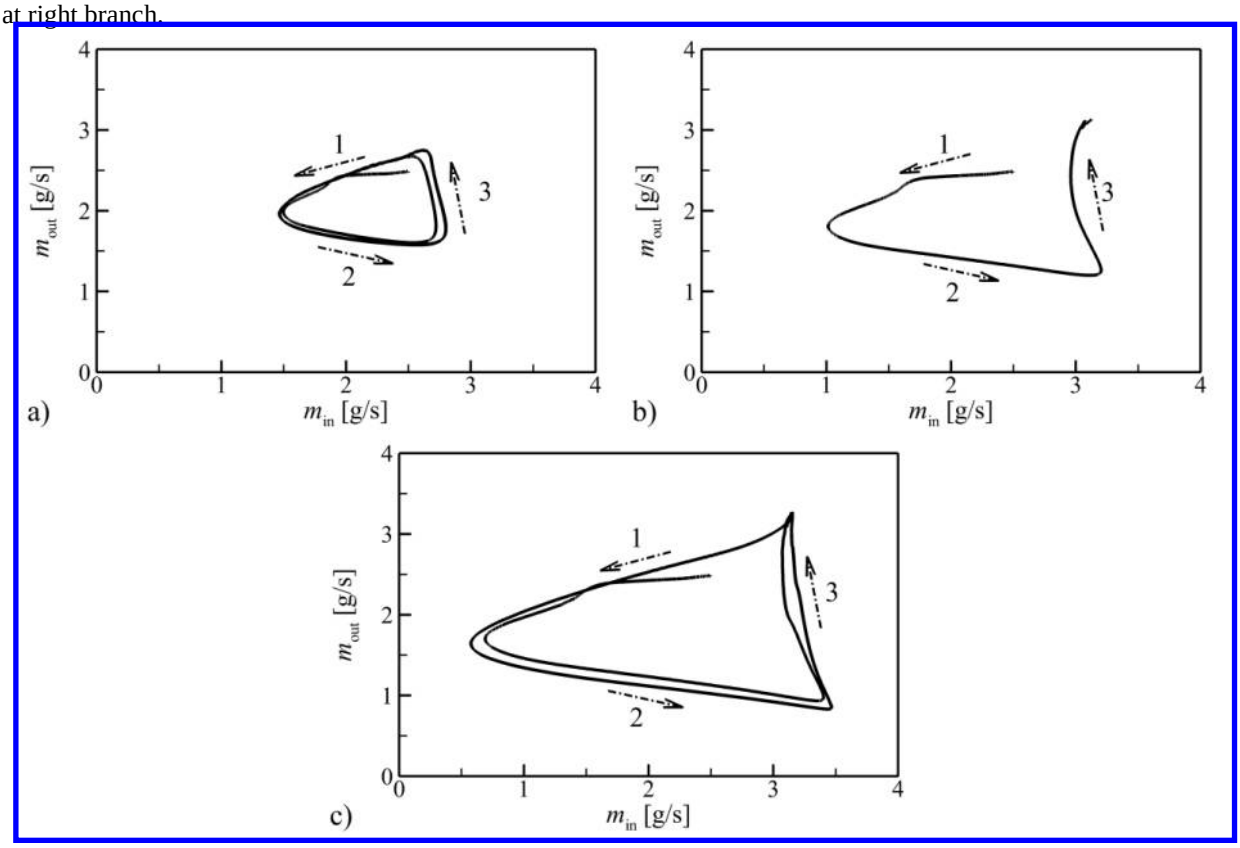


**Fig. 11. The limit cycles under driving pressure drop of a) 10.4 kPa, b) 10.2 kPa and c) 10.1 kPa**

## V. Conclusions

To deepen the understanding of the flow characteristics of supercritical hydrocarbon fuels in the regenerative cooling system, this paper developed a one-dimensional transient simulation model. The reliability of the model was validated against the associated experiments and existing numerical simulations, then the effect of external driving pressure drop on the flow evolution was thoroughly discussed. The main conclusions are as follow:

1) The calculated results in this paper are in good agreement with the relevant experimental data, which indicates that the present transient model is reliable to study the problem of flow instability in the cooling channels using hydrocarbon fuels. By exploiting this model, it is helpful to deepen the understanding of the mechanism of flow instability for the hydrocarbon flow under supercritical condition in the cooling channels.

2) Through a serial of transient simulations, it is observed that the operating point in the right branch is stable, while the one working in the negative slope region is unstable, which is consistent with the prediction obtained with steady state linear stability analysis.

3) The flow is more complex in the left branch. As the external driving force decreases, it can be divided into several scenarios. a) When the operating point is close to the maximum point, the flow in the cooling channel is stable. b) The flow pattern transforms from stable node to a limit cycle with a constant-oscillation amplitude. Besides, as the external pressure drop decreases, the amplitude increases but the frequency decreases. c) The flow rate in the channel oscillates from the left equilibrium point to the right one, and finally stabilizes at the right branch. d) The channel flow behaves as a low-frequency oscillation with a relatively large amplitude. Moreover, both the oscillation's amplitude and frequency increase with a decreased external driving pressure drop.

## Acknowledgments

This work was supported by National Key Project (Grant No. GJXM92579). The authors are also grateful to National Supercomputer Center in Tianjin for providing computational resource.

## Reference

1. Shin, C. W., and No, H. C., "Experimental study for pressure drop and flow instability of two-phase flow in the PCHE-type steam generator for SMRs," *Nuclear Engineering and Design*, Vol.318, 2017, pp.109-118. doi: 10.1016/j.nucengdes.2017.04.004
2. Paul, S., "On nuclear-coupled thermal-hydraulic instability analysis of Super-Critical-Light-Water-cooled-reactor (SCLWR)," *Progress in Nuclear Energy*, Vol.117, 2019, 103051. doi: 10.1016/j.pnucene.2019.103051
3. Zhang, T. J., Wen, J. T., Peles, Y., Catano, J., Zhou, R., and Jensen M. K., "Two-phase refrigerant flow instability analysis and active control in transient electronics cooling systems," *International Journal of Multiphase Flow*, Vol.37, No.1, 2011, pp.84-97. doi: 10.1016/j.ijmultiphaseflow.2010.07.003
4. Yang, Z. Q., Li, T. H., Zhao, X., Gao, T. Z. and Zhang, B.,"Hydrodynamic and heat transfer characteristics of binary hydrocarbons at trans- and supercritical pressures," *Experimental Thermal and Fluid Science*, Vol.116, 2020, 110128. doi: 10.1016/j.expthermflusci.2020.110128
5. A. F. N., and B. M. P., "Pseudo-boiling and heat transfer deterioration while heating supercritical liquid rocket engine propellants," *The Journal of Supercritical Fluids*, Vol.168, 2020, 105066. doi: 10.1016/j.supflu.2020.105066
6. Pan, H., Bi, Q., Liu, Z., Song, F., and Fan, F., "Experimental investigation on thermo-acoustic instability and heat transfer of supercritical endothermic hydrocarbon fuel in a mini tube," *Experimental Thermal and Fluid Science*, Vol.97, 2018, pp.109-118. doi: 10.1016/j.expthermflusci.2018.03.017
7. Ledinegg, M., "Instability of flow during natural and forced circulation," Die Waerme,Vol. 61, No.8, 1938, pp.891–898.
8. Padki, M. M., Palmer, K., Kaka, S., and Veziroglu, T. N., "Bifurcation analysis of pressure-drop oscillations and the Ledinegg instability," *International Journal of Heat and Mass Transfer*, Vol,35, No.2, 1992, pp.525-532. doi: 10.1016/0017-9310(92)90287-3
9. Ghione, A., Noel, B., Vinai, P., and Demaziere, C., "Criteria for Onset of Flow Instability in heated vertical narrow rectangular channels at low pressure: An assessment study," *International Journal of Heat and Mass Transfer*, Vol.105, 2017, pp.464-478. doi: 10.1016/j.ijheatmasstransfer.2016.10.012
10. Kakac, S., and Bon, B., "A Review of two-phase flow dynamic instabilities in tube boiling systems," *International Journal of Heat and Mass Transfer*, Vol.51,No.3-4, 2008, pp.99-433. doi: 10.1016/j.ijheatmasstransfer.2007.09.026
11. Singh, M. P., and Singh, S., "Non-linear stability analysis of supercritical carbon dioxide flow in inclined heated channel," *Progress in Nuclear Energy*, Vol.117, 2019, 103048. doi: 10.1016/j.pnucene.2019.103048
12. Schlichting, W. R., Laheyjr, R. T., and Podowski M. Z., "An analysis of interacting instability modes, in a phase change system," *Nuclear Engineering and Design*, Vol.240, No.10, 2010, pp.3178-3201. doi: 10.1016/j.nucengdes.2010.05.058
13. Munoz-Cobo, J. L., Podowski, M. Z., and Chiva S., "Parallel channel instabilities in boiling water reactor systems: boundary conditions for out of phase oscillations," *Annals of Nuclear Energy*, Vol.29, No.16, 2002, pp.1891-1917. doi: 10.1016/S0306-4549(02)00024-5
14. Lee, J. D., and Pan, C., "Dynamics of multiple parallel boiling channel systems with forced flows," *Nuclear Engineering and Design*, Vol.12, No.1, 1999, pp.31-44. doi: 10.1016/S0029-5493(99)00085-0
15. Yun, G., Qiu, S. Z., Su, G. H., and Jia, D. N., "The influence of ocean conditions on two-phase flow instability in a parallel multi-channel system," *Annals of Nuclear Energy*, Vol.35, No.9, 2008, pp.1598-1605. doi: 10.1016/j.anucene.2008.03.003
16. Chen, J., Gu, H., and Xiong, Z.,"Development of one-dimensional transient model for predicting flow instability at supercritical pressures," *Progress in Nuclear Energy*, Vol.112, 2019, pp.162-170. doi: 10.1016/j.pnucene.2018.12.014
17. Lu, X., Wu, Y., Zhou, L., Tian, W., Su, G., Qiu, S., and Hong, Z., "Theoretical investigations on two-phase flow instability in parallel channels under axial non-uniform heating," *Annals of Nuclear Energy*, Vol.63, 2014, pp.75-82. doi: 10.1016/j.anucene.2013.07.030
18. Ruspini, L. C., Dorao, C. A., and Fernandino, M., "Dynamic simulation of Ledinegg instability," *Journal of Natural Gas Science and Engineering*, Vol.2, No.5, 2010, pp.211-216. doi: 10.1016/j.jngse.2010.08.003
19. Incropera, F., DeWitt, D., "Introduction to Heat Transfer", third ed., John Wiley &Sons, New York, 1996.
20. Zhang S., Zhao X., Bayyuk S., "Generalized formulations for the Rhie–Chow interpolation," *Journal of Computational Physics*, Vol.258, No.1, 2014, pp.880-914. doi: 10.1016/j.jcp.2013.11.006
21. Xiong T., Yan X., Huang S. F., Yu J. C. and Huang Y. P."Modeling and analysis of supercritical flow instability in parallel channels," *International Journal of Heat and Mass Transfer*, Vol.35, 2013, pp.549-557. doi: 10.1016/j.ijheatmasstransfer.2012.08.046
22. Ward, T., Ervin. J. S., Striebich, R. C., and Zabarnick S., "Simulations of Flowing Mildly-Cracked Normal Alkanes Incorporating Proportional Product Distributions," *Journal of Propulsion and Power*, Vol.20, No.2, 2004, pp.394-402. doi: 10.2514/1.10380
23. Liu, F., Lv, J., Zhang, B., and Yang, Z.," Nonlinear stability analysis of Ledinegg instability under constant external driving force," *Chemical Engineering Science*, Vol.206, 2019, pp.432-445. doi: 10.1016/j.ces.2019.05.035

24. Ruan, B., Huang, S. Z., Meng, H., and Gao, X. W.,."Transient responses of turbulent heat transfer of cryogenic methane at supercritical pressures," *International Journal of Heat and Mass Transfer*, Vol.109, 2017, pp.326-335. doi: 10.1016/j.ijheatmasstransfer.2017.02.006

.